PHYSICAL REVIEW D VOLUME 36, NUMBER 5 1 SEPTEMBER 1987

Deep-inelastic structure functions in the MIT bag model

Charles J. Benesh and Gerald A. Miller
Institute for Nuclear Theory, Department of Physics, FM-15, University of Washington, Seattle, Washington 98195
(Received 9 March 1987)

Deep-inelastic structure functions are calculated from a Peierls-Yoccoz-projected MIT bag wave function. The calculation yields quark distribution functions that have the correct support as a function of Bjorken x. These functions are evolved to $Q^2=15$ GeV^2 using QCD perturbation theory, where they are shown to disagree with experiment. Possible improvements are discussed.

I. INTRODUCTION

Since the discovery in 1982 of the European Muon Collaboration (EMC) effect,[1] much effort has been made to understand the effects of the nuclear medium on the quark distributions of individual nucleons.[2] Usually, the starting point for investigations of this type is an empirical determination of the quark distribution of a free nucleon. One then selects a parametrization of the desired nuclear effects and calculates the quark distributions in nuclei. Unfortunately, there is little theoretical understanding of the free-nucleon structure functions $[F_i(x)]$, so choosing the parametrization of the nuclear effects is very difficult. Our opinion is that this lack of knowledge of $F_i(x)$ is responsible for the current confusion about the origins of the EMC effect. Thus, there is renewed interest in the development of techniques for calculating quark distribution functions from nonperturbative quark models. Furthermore, $F_i(x)$ is a fundamental measurable quantity which deserves theoretical attention.

This paper will report on recent progress toward the calculation of quark distributions in the MIT bag model. Previous calculations of this type suffer either from the lack of translational invariance of the bag wave functions,[3] or from the assumptions necessary to ensure momentum conservation.[4,5] Here we use a Peierls-Yoccoz-projected MIT bag wave function for the nucleon and calculate the Bjorken limit of the current-current correlation function. These distributions are interpreted as the twist-two piece of the nucleon structure function evaluated at a low-momentum scale $Q^2=\mu_0^2\simeq 0.5$ GeV^2. QCD perturbation theory is then used to evolve the distributions to $Q^2=15$ GeV^2, where higher-twist effects are small, and comparison with experiment is made.

II. INTERPRETATION OF QUARK-MODEL CALCULATIONS

In the calculations that follow, we shall adopt a point of view suggested by Jaffe and Ross.[4] In particular, we shall assume that the calculations of structure functions in the bag represent the twist-two piece of the physical structure function evaluated at a low value of $Q^2=\mu_0^2$. The motivation for this is the observation from QCD that the quark structure of the nucleon changes with the scale Q^2 at which one probes it. Thus, if the nucleon looks like three valence quarks in a confining interaction at some scale μ_0^2, radiative QCD corrections will change its composition at higher Q^2. Quarks will radiate gluons and these in turn will pair produce quarks until the nucleon becomes a very complicated object.

Knowing the twist-two piece of the structure function at $Q^2=\mu_0^2$, we may then use QCD perturbation theory to evolve to high Q^2. At high enough Q^2, higher-twist effects become negligible and we may compare the resulting distribution functions with data. Note that this prescription implies that the structure functions calculated at $Q^2=\mu_0^2$ should not look like *any* data, since the physical structure function will certainly have important contributions from all twists at this scale.

Finally, we need to decide upon a reasonable value for μ_0^2. Jaffe and Ross[4] determine μ_0^2 by performing a fit of the ratios of evolved and unevolved moments to the predictions of second-order QCD. Here, we will simply require that μ_0^2 be a scale characteristic of a single nucleon. In the bag model, there is only one scale, the bag radius. Hence, we shall take $\mu_0^2\simeq 1/R^2\sim 0.5$ GeV^2. Since QCD evolution depends on μ_0^2 only logarithmically, the precise value of μ_0^2 is not critical to our results. Indeed, we shall see later that varying μ_0^2 by 20% produces little change in our quark distributions.

III. CALCULATION OF STRUCTURE FUNCTIONS

In this section we obtain the distribution functions that serve as boundary conditions for QCD evolution. We wish to calculate the Bjorken limit of

$$W_{\mu\nu}\equiv\frac{1}{4\pi}\int d^4\xi\, e^{+iq\xi}\langle N,\mathbf{p}=\mathbf{0}\,|\,[J_\mu(\xi),J_\nu(0)]\,|\,N,\mathbf{p}=\mathbf{0}\rangle\,, \tag{1}$$

where $|N,\mathbf{p}=\mathbf{0}\rangle$ is the ground state of a nucleon at rest and $J_\mu(x)=\bar\psi(x)\gamma_\mu\psi(x)$ is the usual vector-current operator. [For our purposes, the charge in $J_\mu(x)$ is irrelevant.]

Making the usual parton-model assumptions and taking the Bjorken limit [$q^2\to\infty$, $x=-q^2/2p\cdot q$ fixed, $P_\mu=(M_N,\mathbf{0})$], Eq. (1) reduces to[6]

$$W_{\mu\nu}=\left[\frac{q_\mu q_\nu}{q^2}-g_{\mu\nu}\right]F_1(x)+\left[p_\mu-\frac{p\cdot q}{q^2}q_\mu\right]\left[p_\nu-\frac{p\cdot q\, q_\nu}{q^2}\right]\frac{F_2(x)}{p\cdot q}\ , \tag{2}$$

where

$$\begin{aligned}
&F_1(x)=\frac{1}{2x}F_2(x)\ ,\\
&F_1(x)=\sum_{i=u,d}x[q_i(x)+\bar{q}_i(x)]\ ,\\
&q_i(x)=\frac{1}{4\pi}\int d\xi^- e^{iq^+\xi^-}\langle N,\mathbf{p}=0\,|\,\bar{\psi}_i(\xi^-)\gamma^+\psi_i(0)\,|\,N,\mathbf{p}=0\rangle_c\,\Big|_{\xi^\dagger=\xi_\perp=0}\ ,\\
&\bar{q}(x)=\frac{-1}{4\pi}\int d\xi^- e^{iq^+\xi^-}\langle N,\mathbf{p}=0\,|\,\bar{\psi}_i(0)\gamma^+\psi_i(\xi^-)\,|\,N,\mathbf{p}=0\rangle_c\,\Big|_{\xi^\dagger=\xi_\perp=0}\ ,\\
&\xi^\pm=\frac{\xi^0\pm\xi^3}{\sqrt{2}},\quad q^+=\frac{-Mx}{\sqrt{2}},\quad \gamma^+=\frac{\gamma^0+\gamma^3}{\sqrt{2}}\ .
\end{aligned} \tag{3}$$

In order to proceed further, we must specify the nucleon wave function. We choose a Peierls-Yoccoz-projected version of the usual MIT bag ground state:

$$|\,N,\mathbf{p}=\mathbf{0}\rangle=\lambda\int d^3a\,|\,\mathbf{R}=\mathbf{a}\rangle\ ,$$

where

$$|\,\mathbf{R}=\mathbf{a}\rangle\equiv b_0^\dagger(\mathbf{a})b_0^\dagger(\mathbf{a})b_0^\dagger(\mathbf{a})\,|\,EB;\mathbf{R}=\mathbf{a}\rangle$$

is an unprojected MIT bag state centered at $\mathbf{R}=\mathbf{a}$, $b_0^\dagger(\mathbf{a})$ is the creation operator for the lowest quark mode, and $|\,EB;\mathbf{R}=\mathbf{a}\rangle$ is an empty bag state centered at $\mathbf{R}=\mathbf{a}$. (Flavor-spin and color indices are not made explicit.) The factor λ is chosen so that the state $|\,N,\mathbf{p}=0\rangle$ satisfies the covariant normalization for momentum eigenstates:

$$\lambda^2\equiv\frac{2M}{\int d^3a\langle\mathbf{R}=\mathbf{0}\,|\,\mathbf{R}=\mathbf{a}\rangle}\ . \tag{4}$$

The advantage of this state is that it is an exact eigenstate of momentum. Thus, problems related to translational invariance will not arise. Potential problems are the fact that $|\,N\mathbf{p}=\mathbf{0}\rangle$ is not an exact eigenstate of energy and determining what mass appears in the expression for λ. We address both of these issues below.

To obtain the mass M, we perform a variational calculation of

$$\langle H_{\rm MIT}\rangle=\frac{\langle N,\mathbf{p}=\mathbf{0}\,|\,H_{\rm MIT}\,|\,N,\mathbf{p}=\mathbf{0}\rangle}{\langle N,\mathbf{p}=\mathbf{0}\,|\,N,\mathbf{p}=\mathbf{0}\rangle}\ . \tag{5}$$

Minimizing $\langle H_{\rm MIT}\rangle$ with respect to the bag radius R, we obtain an approximate solution for the ground state and mass. The details of this procedure are given in Appendix A.

Now, we turn to the calculation of the matrix elements in Eq. (3):

$$\begin{aligned}
\mathcal{M}&=\langle N,\mathbf{p}=\mathbf{0}\,|\,\bar{\psi}(\xi)\gamma^+\psi(0)\,|\,N,\mathbf{p}=\mathbf{0}\rangle\\
&=\lambda^2\int d^3a\,d^3b\langle\mathbf{R}=\mathbf{a}\,|\,\bar{\psi}(\xi)\gamma^+\psi(0)\,|\,\mathbf{R}=\mathbf{b}\rangle_c\ .
\end{aligned} \tag{6}$$

Expand the field operator on the right-hand side in terms of MIT bag states centered at $\mathbf{R}=\mathbf{b}$, those on the left-hand side in terms of MIT bag states centered at $\mathbf{R}=\mathbf{a}$:

$$\begin{aligned}
\psi(\mathbf{x},t)=\sum_{n,\kappa}[\,&b_{n,\kappa}(\mathbf{a})\phi_{n,\kappa}(\mathbf{x}-\mathbf{a})e^{-i\omega_{n\kappa}t/R_0}\\
&+d^\dagger_{n,\kappa}(\mathbf{a})\tilde{\phi}_{n,\kappa}(\mathbf{x}-\mathbf{a})e^{i\omega_{n\kappa}t/R_0}]\ ,
\end{aligned} \tag{7}$$

where $b^\dagger_{n,\kappa}(\mathbf{a})$ and $d^\dagger_{n,\kappa}(\mathbf{a})$ create quark and antiquark excitations with wave functions $\phi_{n,\kappa}(\mathbf{a})$ and $\tilde{\phi}_{n,\kappa}(\mathbf{x}-\mathbf{a})$.

The wave functions are given by

$$\phi_{n\kappa}(\mathbf{x})=\frac{N_{n\kappa}}{\sqrt{4\pi}}\begin{bmatrix} j_0(\omega_{n\kappa}\,|\,\mathbf{x}\,|\,/R_0) & U_M\\ i\boldsymbol{\sigma}\cdot\hat{\mathbf{x}}j_1(\omega_{n\kappa}\,|\,\mathbf{x}\,|\,/R_0) & U_M\end{bmatrix}\theta(R_0-n)\ , \tag{8}$$

where $j_l(z)$ are spherical Bessel functions, U_M are two-component Pauli spinors, and $N_{n\kappa}$ is a normalization constant.

Finally, we need to specify the anticommutation relations[7] between the creation and annihilation operators in (7):

$$\begin{aligned}
\{b_n^\dagger(\mathbf{a}),b_m(\mathbf{b})\}&=\int d^3r\,\phi_n^\dagger(\mathbf{r}-\mathbf{a})\phi_m(\mathbf{n}-\mathbf{b})\\
&\equiv\Delta_{nm}(\mathbf{b}-\mathbf{a})\ ,\\
\{d_n^\dagger(\mathbf{a}),d_m(\mathbf{b})\}&=\int d^3r\,\tilde{\phi}_n^\dagger(\mathbf{r}-\mathbf{a})\tilde{\phi}_M(\mathbf{n}-\mathbf{b})\\
&\equiv\Delta_{nm}(\mathbf{b}-\mathbf{a})\ .
\end{aligned} \tag{9}$$

Since we deal only with the lowest quark modes, we use the following notations:

$$\begin{aligned}
&\omega_{0,-1}\equiv\epsilon=2.04,\quad \phi_{0,-1}(\mathbf{x})=\phi_0(\mathbf{x})\ ,\\
&N_{0,-1}\equiv N,\quad \Delta_{00}(\mathbf{z})=\Delta(\mathbf{z})\ .
\end{aligned} \tag{10}$$

We use the expansion (7) to obtain $\mathcal{M}$ of Eq. (6). Then it is simple to show that

$$\mathcal{M}=18\lambda^2\int d^3a\,d^3b\,\Delta^2(\mathbf{b}-\mathbf{a})\bar{\phi}_0(\xi-\mathbf{a})\gamma^+\phi_0(-\mathbf{b})e^{-i\epsilon\xi_0/R_0}\langle EB;\mathbf{R}=\mathbf{a}\,|\,EB;\mathbf{R}=\mathbf{b}\rangle\ . \tag{11}$$

The $\Delta^2(\mathbf{b}-\mathbf{a})$ term enters as a result of applying the anticommutation relations. In Appendix B, we show that this reduces to

$$\mathcal{M}=18\lambda^2N^2\int\frac{d^3K}{(2\pi)^3}\exp\left[-i\left[\frac{\epsilon\xi^0}{R_0}-\mathbf{K}\cdot\xi\right]\right]\tilde{F}(\mathbf{K})\bar{\tilde{\phi}}(\mathbf{K})\gamma^+\tilde{\phi}_0(\mathbf{K}) , \tag{12}$$

where

$$\tilde{F}(\mathbf{K})=\int d^3z\, e^{-i\mathbf{K}\cdot\mathbf{z}}\Delta^2(\mathbf{z})\langle EB;\mathbf{R}=\mathbf{z}\,|\,EB;\mathbf{R}=\mathbf{0}\rangle ,$$

$$\tilde{\phi}_0(\mathbf{K})=\int d^3z\, e^{-i\mathbf{K}\cdot\mathbf{z}}\phi_0(\mathbf{z}) .$$

Plugging this result into Eq. (3) yields

$$q(x)=\frac{\sqrt{2}}{2}\int_{K_-}^{\infty}\frac{K\,dK}{(2\pi)^3}\tilde{F}(\mathbf{K})\bar{\tilde{\phi}}_0(\mathbf{K})\gamma^+\tilde{\phi}_0(\mathbf{K}) , \tag{13}$$

where $K_-=|Mx-\epsilon/R_0|$.

Putting in the MIT bag wave functions, Eq. (8), we get ($\beta_-\equiv KR_0$)

$$q(x)=\frac{(MR_0)(N^2R_0^3)}{2\pi V}\int_{|\beta_-|}^{\infty}d\beta\,\tilde{G}(\beta)\left[t_0^2(\epsilon,\beta)+t_1^2(\epsilon,\beta)+\frac{2\beta_-}{\beta}t_0(\epsilon,\beta)t_1(\epsilon,\beta)\right] , \tag{14a}$$

where $\beta_-=\epsilon-MR_0x$, and

$$\bar{q}(x)=-\frac{(MR_0)(N^2R_0^3)}{2\pi V}\int_{|\beta_+|}^{\infty}d\beta\,\tilde{G}(\beta)\left[t_0^2(\epsilon,\beta)+t_1^2(\epsilon,\beta)+\frac{2\beta_+}{\beta}t_0(\epsilon,\beta)t_1(\epsilon,\beta)\right] , \tag{14b}$$

where $\beta_+=\epsilon+MR_0x$. The functions appearing in Eqs. (14) and (15) are given by

$$\begin{aligned}
\tilde{G}(\beta)&=\int_0^1 y\,dy\,\sin 2\beta y\Delta^2(y)\langle EB;\mathbf{R}=2R_0y\hat{\mathbf{z}}\,|\,EB;\mathbf{R}=0\rangle ,\\
V&=\int_0^1 y^2dy\,\Delta^3(y)\langle EB;\mathbf{R}=2R_0y\hat{\mathbf{z}}\,|\,EB;\mathbf{R}=0\rangle ,\\
t_0(\epsilon,\beta)&=\int_0^1 y^2dy\,j_0(\epsilon y)j_0(\beta y) ,\\
t_1(\epsilon,\beta)&=\int_0^1 y^2dy\,j_1(\epsilon y)j_1(\beta y) ,
\end{aligned} \tag{15}$$

A problem that is apparent in the analytic expressions is that $\bar{q}(x)<0$. This is a result of improper treatment of the cavity-vacuum bubbles shown in Fig. 1. In the approximation we are using, high-momentum quarks behave as free particles; hence, the graph shown in Fig. 1 is completely disconnected and therefore discarded. Whether or not this is the correct procedure in the bag cannot be determined, since the vacuum state is not included in the model.[8] A lesson to be learned from this is that the sea-quark distributions we have obtained should not be trusted. Hence, we confine our attention to the valence distribution $q_v(x)=q(x)-\bar{q}(x)$. As we shall see below, this distribution satisfies the normalization and momentum constraints to a reasonable approximation.

Lastly, we need to specify the empty-bag–empty-bag matrix elements that appear in the expressions for $q_v(x)$. The bag model gives us no input on this question. We shall assume that these matrix elements are approximately constant in the region where the quark overlap integrals are large. Hence, the matrix elements divide out of the expressions for $q(x)$ and $\bar{q}(x)$. The resulting valence distribution is shown in Fig. 2 along with the analogous unprojected result.

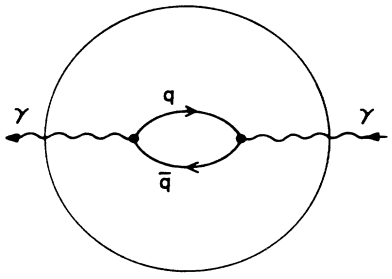

FIG. 1. Cavity-vacuum bubble diagram.

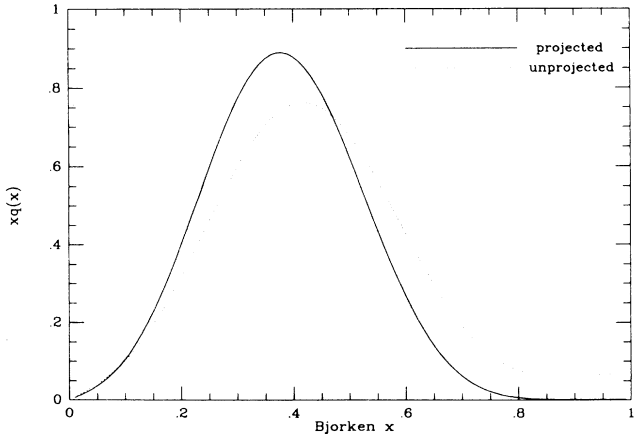

FIG. 2. Valence-quark distributions at the bag scale for projected and unprojected MIT bag.

Results for the case of (1 + 1) dimensions are reported and discussed in Appendix C.

IV. QCD EVOLUTION

The valence-quark distributions calculated in the last section are evolved from $Q^2=\mu_0^2=0.5$ GeV^2 to $Q^2=15$ GeV^2 using second-order QCD perturbation theory,[9] with $\Lambda_{\rm QCD}=150$ MeV. One may ask whether or not perturbation theory may be trusted at such low values of Q^2. Pennington and Ross[10] have argued that not all QCD perturbation expansions need be equally convergent and certain "good" predictions may be obtained, independent of the renormalization scheme, which appear to converge very fast. The nonsinglet evolution equations are an example of such "good" predictions and we hope that it will reliably interpolate between the bag scale μ_0^2 and experiment at high Q^2.

The results of the evolution are shown in Fig. 3 for first ($\mu_0^2=0.5$ GeV^2) and second ($\mu_0^2=0.4$, 0.5, 0.6 GeV^2) order; also shown are data from the CERN-Dortmund-Heidelberg-Saclay (CDHS) Collaboration.[11] The relative smallness ($\sim 10\%$) of the second-order QCD corrections give some credence to the idea that perturbation theory is applicable at the bag scale. One should also note the slow variation of our results with changing μ_0^2.

The oscillations of $q(x)$ for $x \gtrsim 0.7$ are an artifact of approximating the distribution by a ten-term Legendre series. Inclusion of additional terms would suppress these oscillations without affecting the shape of the curve at low x.

V. RESULTS AND CONCLUSION

We begin this section by reviewing the consistency of our calculations. First, we note that the valence quarks are the only objects in the bag that can carry momentum, so the valence quarks should carry all the momentum. In terms of the distribution functions, this means

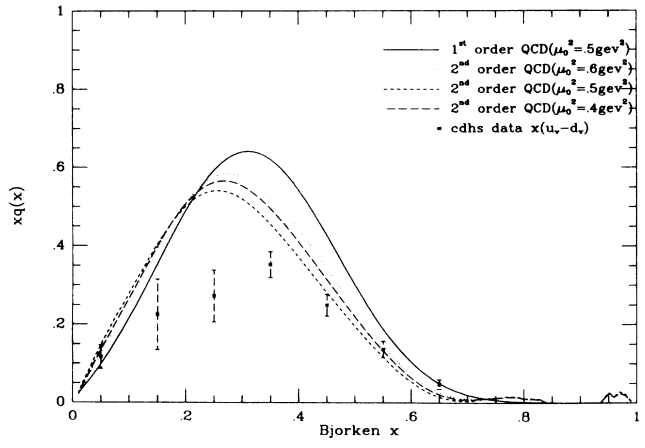

FIG. 3. Results of QCD evolution to $Q^2=15$ GeV^2. The solid curve is first-order evolution ($\mu_0^2=0.5$ GeV^2). The dashed curves are second-order evolution for $\mu_0^2=0.4$, 0.5, 0.6 GeV^2.

$$N\equiv\int_0^1 dx\, q_v(x)=1 \quad \text{and} \quad \langle x\rangle\equiv\int_0^1 dx\, xq_v(x)=\tfrac{1}{3}$$

at the bag scale.

Numerically, we find $N\simeq 1.004$ and $\langle x\rangle\simeq 0.312$. Thus, roughly 6% of the bag's momentum is "missing" in our calculation. There are several possible explanations for this. First, our variational calculation of the bag mass used only one parameter, the bag radius. We show in Appendix B that this leads to $MR_0=4\epsilon$, the same as in the unprojected bag. Inclusion of additional parameters in the nucleon wave function will cause MR to decrease. Since the value of MR_0 determines the scale of x, decreasing MR_0 will increase $\langle x\rangle$.

Another possibility is that our assumption that the bag-bag matrix elements are constant is not quite correct. Modeling these matrix elements by a decreasing function of the bag separation increases the quark distributions at large x, without affecting their normalization. Hence, the momentum fraction $\langle x\rangle$ again increases.

Choosing between these two possibilities is impossible within the context of the MIT bag. These questions may be addressed in a more sophisticated model such as the soliton bag. Here, these considerations serve to check whether our approximations are reasonable. We conclude that they are.

In Fig. 2 we see that the projected calculation has vastly improved support properties when compared with the unprojected result. At $x=1$, the projected quark distributions are 30 times smaller than the unprojected ones and are decreasing more rapidly. Thus, admixtures of mass states other than the ground state are quite small.

Comparison of the evolved valence distributions with experimental data gives no agreement at all. The calculated values of $xq_v(x)$ are roughly a factor of 2 larger than experiment. This may have been anticipated before any calculations were made. To see this, consider the following argument:[12] In *any* model that contains only valence quarks, those quarks must carry all the momentum in the bag. If we associate the scale $\mu_0^2\simeq 0.5$ GeV^2 with this model, then evolution to 10 GeV^2 will give valence-quark distributions that carry momentum fraction[13]

$$\langle x\rangle=\frac{1}{3}\left[\frac{\ln\mu_0^2/\Lambda_{\rm QCD}^2}{\ln Q^2/\Lambda_{\rm QCD}^2}\right]^{0.395}=0.255$$

with $\Lambda_{\rm QCD}=150$ MeV.

Experimentally,[14] one finds $\langle x\rangle=0.155$ for u quarks, and $\langle x\rangle=0.12$ for d quarks. Since $\langle x\rangle$ is simply the area under the curve $xq_v(x)$, we see that *any* quark-model calculation will yield valence distributions roughly twice as large as experiment.

A simple solution to this difficulty is to choose a different value for μ_0^2 such that $\langle x\rangle$ agrees with experiment at high Q^2. Using second-order QCD, we determine this value of μ_0^2 to be around 0.1 GeV^2. In terms of distances, this corresponds to about $2.2R_N$. This distance scale seems too large to be associated with the physics of a single nucleon. Furthermore, the perturbative analysis for the moments is not trustworthy at this scale.

A more realistic possibility, we feel, is to keep $\mu_0^2\simeq 0.5$ GeV^2 and to add new components to the nucleon wave

function. These new dynamical variables carry momentum, and the right combination may be found to reproduce the data. Among the possibilities for these new degrees of freedom are pions, sea quarks, collective oscillations of the bag surface, and explicit gluons in the bag wave function. Work on these topics is currently in progress.

In conclusion, we stress that the quark distributions we have calculated have, to a very good approximation, the support properties required by energy-momentum conservation. Thus, they provide a foundation for further calculations of quark distributions in nucleons and, once that is complete, nuclei.

APPENDIX A: DETERMINATION OF THE PROJECTED STATE'S MASS

We determine the mass of the projected bag state by a simple variational calculation. We begin with the Hamiltonian

$$H_{\rm MIT}=\int_v d^3r\left[\frac{1}{i}\psi^\dagger\boldsymbol{\alpha}\cdot\nabla\psi+B\right]+\text{constraint} . \quad \text{(A1)}$$

Our trial wave functions for the quarks satisfy the constraint condition by construction. Hence, we shall ignore the constraint term in what follows.

Consider first the quark kinetic-energy term. This term is translationally invariant; hence, it gives the same contribution as the unprojected case:

$$\langle E_K\rangle=\frac{3\epsilon}{R} . \quad \text{(A2)}$$

The remaining term involves the following matrix element:

$$\langle N,\mathbf{p}=\mathbf{0}\mid v\mid N,\mathbf{p}=\mathbf{0}\rangle ,$$

where v is the bag's volume operator. By dimensional analysis, this matrix element must be proportional to R^3. Therefore,

$$\langle H_{\rm MIT}\rangle=\frac{3\epsilon}{R}+4\pi\alpha BR^3 ,$$

where $\alpha<1$ is a numerical constant.

Taking $\delta\langle H_{\rm MIT}\rangle/\delta R=0$, we find $4\pi\alpha BR^3=\frac{1}{3}(3\epsilon/R)$. Thus, the relation between the mass and radius of the bag is the same as in the unprojected case, i.e., $MR=4\epsilon$. Note, however, that the radius differs from the unprojected radius by a factor of $\alpha^{-1/4}$ so that the mass is lower than the unprojected mass.

APPENDIX B: EVALUATION OF MATRIX ELEMENT

We begin with Eq. (2) of the text

$$\mathcal{M}=18\lambda^2\int d^3a\,d^3b\,N^2\Delta^2(\mathbf{a}-\mathbf{b})\bar{\phi}_0(\xi-\mathbf{a};0)\gamma^+\phi_0(-\mathbf{b},0)e^{-i\epsilon\xi_0/R_0} . \quad \text{(B1)}$$

The empty-bag–empty-bag matrix element must be a function of $\mathbf{a}-\mathbf{b}$; hence, we introduce the functions

$$\tilde{F}(\mathbf{k})=\int d^3z\,e^{-i\mathbf{k}\cdot\mathbf{z}}\Delta^2(\mathbf{z})\langle EB;\mathbf{R}=\mathbf{z}\mid EB;\mathbf{R}=\mathbf{0}\rangle , \quad \tilde{\phi}_0(\mathbf{k})=\int d^3z\,e^{-i\mathbf{k}\cdot\mathbf{z}}\phi_0(\mathbf{z},0) .$$

Inverting the Fourier transforms we find

$$\mathcal{M}=18\lambda^2N^2\int d^3a\,d^3b\int\frac{d^3k_1d^3k_2d^3k_3}{(2\pi)^9}e^{i\mathbf{k}_1\cdot(\mathbf{a}-\mathbf{b})}e^{-i\mathbf{k}_2\cdot(\xi-\mathbf{a})}e^{-i\mathbf{k}_3\cdot\mathbf{b}}\tilde{\phi}_0(\mathbf{k}_2)\gamma^2\phi_0(\mathbf{k}_3)e^{-i\epsilon\xi_0/R_0}$$

$$=18\lambda^2N^2\int\frac{d^3k_1}{(2\pi)^3}e^{-i(\epsilon\xi_0/R_0-\mathbf{k}_1\cdot\xi)}\tilde{F}(\mathbf{k}_1)\bar{\tilde{\phi}}_0(\mathbf{k}_1)\gamma^+\phi_0(\mathbf{k}_1) ,$$

where we have switched $\mathbf{k}_1\leftrightarrow-\mathbf{k}_1$ and used the rotational invariance of $\tilde{F}(\mathbf{k}_1)$.

APPENDIX C: COMPARISON OF TRANSLATIONALLY INVARIANT STRUCTURE FUNCTIONS IN 1+1 DIMENSIONS

In $1+1$ dimensions, exact translationally invariant solutions of the MIT bag are known.[15] Severe ordering ambiguities in the quark field operators prevent one from making exact calculations of structure functions. Jaffe[16] has calculated structure functions in the "L_0 approximation," in which the bag is a static cavity of fixed length on the light cone. In this approximation, the correlation functions are simply related to those of the static-cavity model, i.e.,

$$F(x)\equiv\lim_{Bj}\int\frac{d^2x}{4\pi}e^{iqx}\langle T\mid\bar{\psi}(x)\psi(x)\bar{\psi}(0)\psi(0)\mid T\rangle \quad \text{(C1)}$$

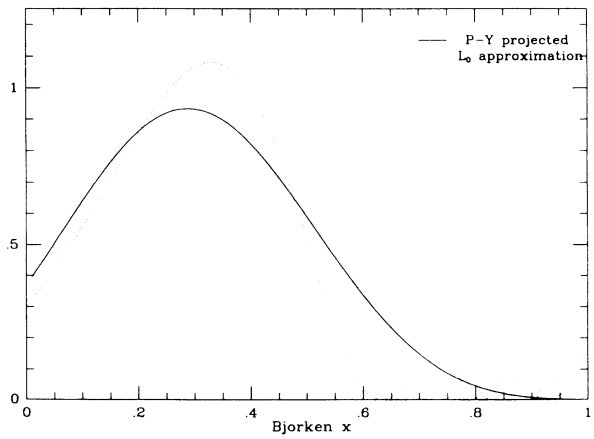

FIG. 4. Structure functions of the two-dimensional MIT bag with three quarks.

with

$$F_{L_0}(x)=\frac{F_{\rm SC}(-\ln(1-x))}{1-x} , \tag{C2}$$

where $F_{L_0}(x)$ is the correlation function in the L_0 approximation, and $F_{\rm SC}(x)$ is obtained from (C1) using the standard static-cavity approximation.

The correlation function defined above may also be calculated using the Peierls-Yoccoz ansatz described in the text. The result is

$$F_{\rm PY}(x)=\frac{I_2(x)}{I_3}F_{\rm SC}(x) ,$$

where

$$I_1(x)\equiv\int_0^1 dz\cos^2\left[\frac{\pi z}{2}\right](1-z)^2\cos[(ML x-\pi/2)z] ,$$

$$I_3\equiv\int_0^1 dz\cos^3\left[\frac{\pi z}{2}\right](1-z)^3 .$$

The distributions obtained by both these approximations are shown in Fig. 4. Qualitatively, the results are very similar. The only difference is the oscillatory behavior of the L_0 distributions at large x. We believe that these oscillations are an artifact of the sharp bag surface in this approximation. It is encouraging that these two approximations do not give very different results.

[1]J. J. Aubert *et al.*, Phys. Lett. **123B**, 275 (1983); A. Bodek *et al.*, Phys. Rev. Lett. **50**, 1431 (1983); **51**, 534 (1983); R. G. Arnold *et al.*, *ibid.* **52**, 727 (1984); A. C. Benvenuti *et al.*, in *Proceedings of the 22nd International Conference on High Energy Physics,* Leipzig, 1984, edited by A. Meyer and E. Wieczorek (Akademie der Wissenschaften der DDR, Zeuthen, East Germany, 1984), Vol. 1, p. 219.

[2]For reviews, see R. L. Jaffe, Comments Nucl. Part. Phys. **13**, 39 (1984); C. H. Llewellyn Smith, Nucl. Phys. **A434**, 35c (1985).

[3]R. L. Jaffe, Phys. Rev. D **11**, 1953 (1975).

[4]R. L. Jaffe and G. G. Ross, Phys. Lett. **93B**, 313 (1980).

[5]L. S. Celenza and C. M. Shakin, Phys. Rev. C **27**, 1561 (1983).

[6]For a detailed derivation of this result, see R. L. Jaffe, in *Relativistic Dynamics and Quark Nuclear Physics,* proceedings of the Los Alamos School, 1985, edited by M. B. Johnson and A. Picklesimer (Wiley, New York, 1986).

[7]G. Lübeck, Ph.D. thesis, University of Washington, 1986.

[8]Analogous problems occur in the unprojected version of the bag. See Ref. 3.

[9]The details of this procedure are given in A. J. Buras, Rev. Mod. Phys. **52**, 199 (1980).

[10]M. Pennington and G. G. Ross, Phys. Lett. **86B**, 371 (1979).

[11]H. Abramowicz *et al.*, Z. Phys. C **25**, 29 (1984).

[12]N. N. Nikolaev, Tokyo Report No. INS-Rep-539, 1985 (unpublished).

[13]Inclusion of second-order effects does not alter this result by more than a few percent.

[14]H. Abramowicz *et al.*, Z. Phys. C **17**, 283 (1983).

[15]A. Chodos, R. L. Jaffe, K. Johnson, C. B. Thorn, and V. F. Weisskopf, Phys. Rev. D **9**, 3471 (1974).

[16]R. L. Jaffe, Ann. Phys. (N.Y.) **132**, 32 (1981).